

---

## PASSIVITY-BASED SENSORLESS POSITION-FLUX TRACKING CONTROLLER FOR INDUCTION MOTOR

---

### 1. Introduction

Vector controlled AC drives, based on different types of AC motors, have become the most spread high dynamic performance electromechanical systems [1], [2]. In servo applications the permanent magnet synchronous motor drives have replaced the converter controlled dc motor drives. Nevertheless for wide spectrum of medium performance systems, the synchronous motor drives are quite expensive. Low cost position controlled induction motor drives (with standard machine for inverter control) is an attractive solution for such applications. Removing the LEM current sensors in this case can be viewed as an important task in the overall cost reduction problem. In [3] the authors developed a current sensorless speed control algorithm, designed in stationary reference frame. This control algorithm is too complex for low cost applications. In this paper we propose a new solution, which is simple in implementation, based on passivity approach, leading to natural induction machine field-orientation.

### 2. Induction motor model and control problem statement

The equivalent two-phase model of symmetrical IM, under assumptions of linear magnetic circuits and balanced operating conditions is presented in an arbitrary rotating reference frame (d-q) [2] as

$$\begin{aligned}
\dot{\theta} &= \omega \\
\dot{\omega} &= \mu(\Psi_d i_q - \Psi_q i_d) - T_L/J - v\omega \\
\dot{i}_d &= -\gamma i_d + \omega_0 i_q + \alpha\beta\Psi_d + \beta\omega\Psi_q + u_d/\sigma \\
\dot{i}_q &= -\gamma i_q - \omega_0 i_d + \alpha\beta\Psi_q - \beta\omega\Psi_d + u_q/\sigma \\
\dot{\Psi}_d &= -\alpha\Psi_d + (\omega_0 - \omega)\Psi_q + \alpha L_m i_d \\
\dot{\Psi}_q &= -\alpha\Psi_q - (\omega_0 - \omega)\Psi_d + \alpha L_m i_q \\
\dot{\epsilon}_0 &= \omega_0
\end{aligned} \tag{1}$$

where  $\mathbf{i} = (i_d, i_q)^T$ ,  $\mathbf{\Psi} = (\Psi_d, \Psi_q)^T$ ,  $\mathbf{u} = (u_d, u_q)^T$  denote stator current, rotor flux and control vectors. Subscripts d and q stand for vector components in the (d-q) reference frame,  $\theta, \omega$  are the rotor position and speed,  $T_L$  is the load torque and  $\epsilon_0$  is the angular position of the (d-q) reference frame with respect to a fixed stator reference frame (a-b), where the physical variables are defined. Transformed variables in (1) are given by

$$\begin{aligned}
\mathbf{x}_{dq} &= e^{-j\epsilon_0} \mathbf{x}_{ab} \\
\mathbf{x}_{ab} &= e^{j\epsilon_0} \mathbf{x}_{dq}
\end{aligned} \quad \text{where} \quad e^{j\epsilon_0} = \begin{bmatrix} \cos \epsilon_0 & \sin \epsilon_0 \\ -\sin \epsilon_0 & \cos \epsilon_0 \end{bmatrix}, \tag{2}$$

where  $\mathbf{x}_{yz}$  stands for any two-dimensional vector of IM.

Positive constants related to the electrical and mechanical parameters of the IM are defined in a standard way.  $J$  is the total rotor inertia,  $v$  is the friction coefficient,  $L_m$  is the magnetizing inductance. One pole pair is assumed without loss of generality.

General specification for position-controlled electric drive requires to control the two IM outputs, position and rotor flux modulus, defined as

$$\mathbf{y}_1 = \begin{bmatrix} \theta \\ (\Psi_d^2 + \Psi_q^2)^{1/2} \end{bmatrix} \triangleq \begin{bmatrix} \theta \\ |\Psi| \end{bmatrix} \tag{3}$$

using the two-dimensional stator voltage vector  $\mathbf{u}$  on the basis of measured variables vector  $\mathbf{y} = (\theta, \omega)^T$ .

Let us define  $\mathbf{y}_1^* = (\theta^*, \Psi^*)^T$ , where  $\theta^*$  and  $\Psi^* > 0$  are position and flux reference trajectories. The position and flux modulus tracking errors are

$$\tilde{\theta} = \theta - \theta^*, \quad \tilde{\Psi} = |\Psi| - \Psi^* \tag{4}$$

Following the concept of indirect field orientation [4] we define d and q axis flux tracking errors as

$$\tilde{\Psi}_d = \Psi_d - \Psi^* \cos \theta, \quad \tilde{\Psi}_q = \Psi_q - \Psi^* \sin \theta \tag{5}$$

Note that  $\lim_{t \rightarrow \infty} \tilde{\Psi}_q = 0$  is the condition of asymptotic field orientation. From (4) and (5) it follows that condition

$\lim_{t \rightarrow \infty} (\tilde{\Psi}_d, \tilde{\Psi}_q) = 0$  is equivalent to  $\lim_{t \rightarrow \infty} \tilde{\Psi} = 0$ .

The position-flux tracking problem is formulated as follows. Consider the IM model(1), (2) and assume that:

- A.1. The rotor position and speed are available for measurement.
- A.2. The motor parameters are known and constant.
- A.3. The load torque  $T_L$  is unknown but constant and bounded.

A.4. The position and flux reference trajectories  $\theta^*$ ,  $\psi^* > 0$  are smooth functions with known bounded first three time derivatives and first two time derivatives correspondingly.

Under these assumptions, it is required to design an output feedback controller satisfying the following control objectives:

CO1. Global asymptotic position-flux tracking and asymptotic field orientation, i.e.

$$\lim_{t \rightarrow \infty} \tilde{\theta} = 0, \lim_{t \rightarrow \infty} \tilde{\psi}_d = 0, \lim_{t \rightarrow \infty} \tilde{\psi}_q = 0 \quad (6)$$

with all signals bounded.

CO2. Asymptotic decoupling of the output variables, namely, if  $\tilde{\psi}_d(0) = 0, \tilde{\psi}_q(0) = 0$ , then  $\tilde{\psi}_d(t) = \tilde{\psi}_q(t) \equiv 0, \forall t \geq 0$  and the dynamics of the mechanical error variables is independent of the flux control.

CO3. Linear dynamics of the nominal ( $\tilde{\psi}_d = \tilde{\psi}_q = 0$ ) position subsystem.

The flux-current subsystem is designed first, to satisfy the flux tracking control objective achieving at the same time asymptotic field orientation. Then the mechanical subsystem is designed to ensure the speed-position tracking.

### 3. Current-flux subsystem design

The control objectives of the flux-current controller are:

- to generate the flux vector angle reference trajectory  $\varepsilon_0(t)$ ;

- to design the control voltage vector  $(u_d, u_q)^T$  in order to guarantee globally exponentially stable flux-torque tracking.

Let us define the stator current references  $i_d^*, i_q^*$  and the corresponding current tracking errors

$$\tilde{i}_d = i_d - i_d^*, \tilde{i}_q = i_q - i_q^* \quad (7)$$

The following control algorithm is adopted for IM electrical subsystem:

**- Flux controller**

$$i_d^* = \frac{1}{\alpha L_m} (\alpha \psi^* + \dot{\psi}^*) \quad (8)$$

$$\dot{\varepsilon}_0 = \omega_0 = \omega + \alpha L_m \frac{i_q^*}{\psi^*}$$

**- Current controller**

$$u_d = \sigma (\gamma i_d^* - \omega_0 i_q^* - \alpha \beta \psi^* + \dot{i}_d^*) \quad (9)$$

$$u_q = \sigma (\gamma i_q^* + \omega_0 i_d^* + \beta \omega \psi^* + \dot{i}_q^*)$$

Substituting flux-current control algorithm into (1) the error dynamics of the IM electrical subsystem becomes

$$\dot{\mathbf{x}}_e = \begin{bmatrix} -\gamma & \omega_0 & \alpha\beta & \beta\omega \\ -\omega_0 & -\gamma & -\beta\omega & \alpha\beta \\ \alpha L_m & 0 & -\alpha & \omega_2 \\ 0 & \alpha L_m & -\omega_2 & -\alpha \end{bmatrix} \mathbf{x}_e \triangleq \mathbf{A}_e(t) \mathbf{x}_e \quad (10)$$

where  $\mathbf{x}_e = (\tilde{i}_d, \tilde{i}_q, \tilde{\psi}_d, \tilde{\psi}_q)^T$ ,  $\omega_2 = \omega_0 - \omega$  is the slip angular frequency.

In order to investigate the stability properties of the non-autonomous linear system (10) let us consider the following Lyapunov function

$$V = \frac{1}{2} \mathbf{x}_e^T \mathbf{P} \mathbf{x}_e \quad (11)$$

where  $\mathbf{P} = \mathbf{P}^T > 0$  is solution of the Lyapunov equation  $\mathbf{A}^T(t) \mathbf{P} + \mathbf{P} \mathbf{A}(t) = -\mathbf{Q}$ ,  $\mathbf{Q} = \mathbf{Q}^T > 0$ .

Selecting

$$\mathbf{P} = \begin{bmatrix} \varepsilon/\beta & 0 & \varepsilon & 0 \\ 0 & \varepsilon/\beta & 0 & \varepsilon \\ \varepsilon & 0 & 1 & 0 \\ 0 & \varepsilon & 0 & 1 \end{bmatrix} > 0, \text{ with } \varepsilon < \frac{1}{\beta} \quad (12)$$

derivative of V along the trajectories of (10) becomes

$$\dot{V} = -\frac{\varepsilon R_s}{\beta \sigma} (\tilde{i}_d^2 + \tilde{i}_q^2) - \alpha(1 - \varepsilon\beta)(\tilde{\psi}_d^2 + \tilde{\psi}_q^2) \triangleq -\mathbf{x}_e^T \mathbf{Q} \mathbf{x}_e, \text{ with } \varepsilon = \frac{\alpha L_m}{\gamma} < \frac{1}{\beta} \quad (13)$$

From (11), (12) and (13) using standard Lyapunov stability arguments we conclude that equilibrium point  $\mathbf{x}_e = 0$  of the system (10) is globally exponentially stable, i.e.

$$\|\mathbf{x}_e(t)\| \leq c_1 \|\mathbf{x}_e(0)\| e^{-c_2 t}, \quad (c_1, c_2) > 0 \quad (14)$$

Asymptotic flux tracking and asymptotic field orientation follow directly from the condition (14) satisfying the second part of CO1. In order to show that torque tracking is achieved as well, let us consider the IM torque equation

$$T = \frac{3}{2} \frac{L_m}{L_r} \left[ \psi^* \tilde{i}_q + \tilde{\psi}^* \tilde{i}_q + \tilde{\psi}_d (\tilde{i}_q + \tilde{i}_d) - \tilde{\psi}_q (\tilde{i}_d + \tilde{i}_d) \right] \triangleq T^* + \tilde{T} \quad (15)$$

where  $T^*$  is the torque reference. Defining in (15)

$$\tilde{i}_q^* = \frac{2}{3} \frac{L_r}{L_m} \frac{T^*}{\psi^*} \quad (16)$$

we obtain

$$\tilde{T} = \frac{3}{2} \frac{L_m}{L_r} \left[ \psi^* \tilde{i}_q + \tilde{\psi}_d (\tilde{i}_q + \tilde{i}_d) - \tilde{\psi}_q (\tilde{i}_d + \tilde{i}_d) \right] \quad (17)$$

For bounded  $\psi^*$ ,  $\tilde{\psi}^*$ ,  $T^*$ , current references  $\tilde{i}_q^*$  and  $\tilde{i}_d^*$  are bounded and therefore  $\tilde{T}(t)$  is an exponentially decaying function according to (14), i.e. asymptotic torque tracking is achieved.

**Remark 1.** Current-flux control algorithm given by (8), (9) is based on concept of indirect field orientation, which is flux open-loop control strategy in classical formulation [1]. Flux-current controller proposed is open-loop with respect to current control as well and its stability and robustness properties (see (12) and (13)) are based on the natural stability properties of IM, providing natural indirect field orientation.

**Remark 2.** The torque reference trajectory should be bounded with bounded known first time derivative in order to be implementable using q-axis current control algorithm in (9).

#### 4. Position-speed subsystem design

Using (15), (16) and (17) we present the IM mechanical subsystem in (1) as

$$\begin{aligned} \dot{\theta} &= \omega \\ \dot{\omega} &= \frac{1}{J} \left( \frac{3}{2} \frac{L_m}{L_r} \psi^* \tilde{i}_q^* - Jv\omega - T_L + \tilde{T} \right) \end{aligned} \quad (18)$$

Let us define the speed tracking error as  $\tilde{\omega} = \omega - \omega^*$ , where  $\omega^*$  is the speed reference, generated by position controller, given by

$$\begin{aligned} \omega^* &= \xi_1 + \dot{\theta}^* \\ \dot{\xi}_1 &= -\frac{1}{\tau_1} \xi_1 - \frac{1}{\tau_1} k_\theta \tilde{\theta} \end{aligned} \quad (19)$$

Substituting (19) into first equation of (18), position tracking error dynamics becomes

$$\begin{aligned} \dot{\tilde{\theta}} &= \xi_1 + \tilde{\omega} \\ \dot{\xi}_1 &= -\frac{1}{\tau_1} \xi_1 - \frac{1}{\tau_1} k_\theta \tilde{\theta} \end{aligned} \quad (20)$$

where  $k_\theta > 0$  is the position controller gain and  $\tau_1$  is a time constant of the auxiliary first order filter.

From second equation in (18) the speed controller is designed as

$$\begin{aligned} \tilde{i}_q^* &= \frac{1}{\mu \psi^*} (v\omega^* + \hat{T}_L + \dot{\omega}^* + \xi_2) \\ \dot{\hat{T}}_L &= -k_\omega \tilde{\omega} \\ \dot{\xi}_2 &= -\frac{1}{\tau_2} \xi_2 - \frac{1}{\tau_2} k_\omega \tilde{\omega} \end{aligned} \quad (21)$$

where  $\hat{T}_L$  is the estimate of  $T_L/J$ , such that load estimation error is  $\tilde{T}_L = T_L/J - \hat{T}_L$ ;  $\tau_2$  is the time constant of the speed filter and  $\dot{\omega}^*$  in (21) is computed using position controller equations (19) as

Total position-speed error dynamics is given by

$$\begin{aligned}\dot{\tilde{\theta}} &= \xi_1 + \tilde{\omega} \\ \dot{\xi}_1 &= -\frac{1}{\tau_1}\xi_1 - \frac{1}{\tau_1}k_\theta\tilde{\theta}\end{aligned}\quad (22)$$

$$\begin{aligned}\dot{\tilde{T}}_L &= k_{\omega_i}\tilde{\omega} \\ \dot{\tilde{\omega}} &= -v\tilde{\omega} - \tilde{T}_L + \xi_2 + \tilde{T}/J \\ \dot{\xi}_2 &= -\frac{1}{\tau_2}\xi_2 - \frac{1}{\tau_2}k_\omega\tilde{\omega}\end{aligned}\quad (23)$$

Position loop dynamics (22) is asymptotically stable for  $\forall(k_\theta, \tau_1) > 0$ , the speed loop dynamics (23) can be designed using three tuning parameters of the speed controller: proportional  $k_\omega$  and integral  $k_{\omega_i}$  gains and filter time constant  $\tau_2$ , which can be selected arbitrary small.

The composite error dynamics is given by (22), (23), (17), (10) and can be presented in the form of general nonlinear feedback interconnection of the mechanical (22), (23) and electrical (10) subsystems as

$$\dot{\mathbf{x}}_m = \mathbf{A}_{m1}\mathbf{x}_m + \mathbf{A}_{m2}(\mathbf{x}_e)\mathbf{x}_m + \mathbf{B}_1(t)\mathbf{x}_e + \mathbf{B}_2(\mathbf{x}_e)\mathbf{x}_e \quad (24)$$

$$\dot{\mathbf{x}}_e = \mathbf{A}_e(\mathbf{x}_m, t)\mathbf{x}_e \quad (25)$$

where  $\mathbf{x}_m = (\tilde{\theta}, \xi_1, \tilde{T}_L, \tilde{\omega}, \xi_2)^T$ ,  $\mathbf{A}_{m1}$  is a constant Hurwitz matrix given in (22), (23) with  $\tilde{T} = 0$ , and

$$\mathbf{A}_{m2}(\mathbf{x}_e)\mathbf{x}_m = \begin{bmatrix} 0 & 0 & 0 & \frac{\tilde{\Psi}_d}{\Psi^*} \left( -\frac{1}{\tau_1} [(1-\tau_1)v]\xi_1 + k_\theta\tilde{\theta} \right) - \tilde{T}_L + \xi_2 & 0 \end{bmatrix}^T \quad (26)$$

$$\mathbf{B}_1(t)\mathbf{x}_e = \begin{bmatrix} 0 & 0 & 0 & \left( v\dot{\theta}^* + \frac{\tilde{T}_L}{J} + \ddot{\theta}^* \right) \frac{\tilde{\Psi}_d}{\Psi^*} + \mu\psi^* \tilde{i}_q - \frac{\mu}{\alpha L_m} (\alpha\psi^* + \dot{\psi}^*) \tilde{\psi}_q & 0 \end{bmatrix}^T \quad (27)$$

$$\mathbf{B}_2(\mathbf{x}_e)\mathbf{x}_e = \begin{bmatrix} 0 & 0 & 0 & \mu(\tilde{\psi}_d \tilde{i}_q - \tilde{\psi}_q \tilde{i}_d) & 0 \end{bmatrix}^T. \quad (28)$$

The main features of the system (24), (25) are:

- constant matrix  $\mathbf{A}_{m1}$  is Hurwitz with appropriate design of the speed and position controllers;
- electrical subsystem (25) is globally asymptotically exponentially stable;
- interconnection terms given by (26), (27), (28) have bounded linear/bilinear properties under conditions of assumptions A.3 and A.4.

According to result in [4], the equilibrium point  $(\mathbf{x}_m^T, \mathbf{x}_e^T)^T = 0$  of the composite system (24), (25) is globally exponentially stable. Consequently, position tracking control objective CO.1 is matched with all internal signals bounded. Control objectives CO.2 and CO.3 are achieved since:

- a) if  $\mathbf{x}_e(0) = 0$ , then  $\mathbf{x}_e(t) \equiv 0 \forall t \geq 0$  and nominal speed-position subsystem  $\dot{\mathbf{x}}_m = \mathbf{A}_{m1}\mathbf{x}_m$  is linear and independent of flux-current control;
- b) if  $\mathbf{x}_e(0) \neq 0$ , then subsystem (24) can be viewed as nominal one perturbed by exponentially vanishing perturbation generated by subsystem (25).

## 5. Experimental results

Experimental tests have been performed in order to evaluate the performance of the proposed control algorithm.

The operating sequences, reported in Fig. 1, are the following:

1. the machine is excited during the initial time interval 0-0.11s using a flux reference trajectory starting at  $\psi^*(0) = 0.02\text{Wb}$  and reaching the motor rated value of 0.86Wb with the first and second derivatives equal to 8 Wb/s and 1000 Wb/s<sup>2</sup> correspondingly;
2. the motor is required to track the position reference trajectory, characterized by the following phases: starting at  $t=0.5$  s from zero initial value, position reference reaches the position of 60 rad; from  $t= 1.15$  s to  $t= 1.7$  s position reference is maintained constant, from  $t= 1.7$  s to  $t=2.35$  s the motor is required to return to 0 rad. Maximum absolute values of the speed reference and of its first and second derivatives are equal to 100 rad/s, 2000 rad/s<sup>2</sup>,  $2 \times 10^5$  rad/s<sup>3</sup> correspondingly;
3. from time  $t=0.7$  s to  $t=0.9$  s, from  $t=1.3$  s to  $t=1.5$  s and from  $t=1.9$  s to  $t=2.1$  s a constant load torque, equal to 100% of the motor rated value (7.0 Nm), is applied. During other time intervals load torque is set to zero.

Referring to (22), (23), the controller parameters can be grouped into two sets: position and speed controller gains  $k_\theta, k_\omega, k_{\omega_i}$  and time constants  $\tau_1, \tau_2$ .

Considering the ideal case of  $\tau_1 = \tau_2 = 0$ , mechanical error dynamics is composed by the 1<sup>st</sup> order position dynamics cascaded with the 2<sup>nd</sup> order speed dynamics.

The parameters of the speed subsystem  $k_\omega, k_{\omega i}$  are tuned accordingly to standard tuning relations

$$1/\tau^2 = k_{\omega i} \text{ and } k_{\omega i} = (k_\omega^2/2)(\delta = 0.707) \text{ or } k_{\omega i} = (k_\omega/2)^2 (\delta = 1)$$

where  $\tau$  and  $\delta$  are the time-constant and damping factor of the second-order speed error subsystem. Position controller gain  $k_\theta$  is set in order to impose the bandwidth of the position control loop. Time constants  $\tau_1, \tau_2$  are set sufficiently small in order to obtain time-scale separation between 3<sup>rd</sup> order position and speed controller and 2<sup>nd</sup> order filters.

In the experiments, the controller tuning parameters are set as follows:  $k_\theta = 60$ ,  $k_\omega = 160$ ,  $k_{\omega i} = 12800$ ,  $\tau_1 = 0.001\text{s}$ ,  $\tau_2 = 0.001\text{s}$ .

Tracking of the position reference trajectory adopted requires a dynamic torque that is equal to the rated value of the motor. Flux and position reference trajectories are presented in Fig. 1 using solid lines; dashed line in the same figure represents the load torque profile.

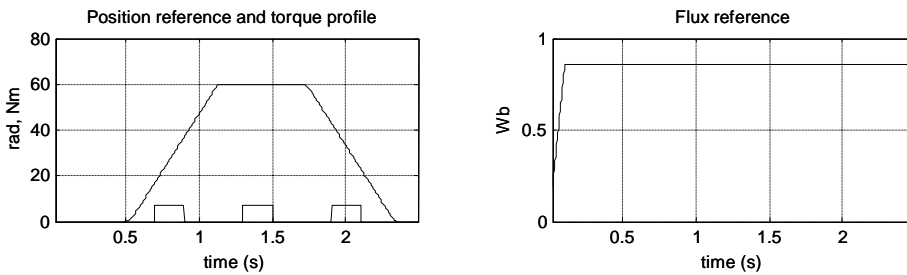


Fig. 1. Position flux references and load torque profile

(DSP) board (based on TMS320C32) directly connected to the PC bus. The DSP board performs data acquisition (eight 12-bit A/D data channels plus two interfaces for incremental encoder), implements control algorithms and generates the PWM signals (two symmetrical three-phase PWM modulator with programmable dead time);

3. a 50A/ 380  $V_{RMS}$  three-phase inverter, operated at 10kHz switching frequency during experiments. Dead time of the inverter is set to 1.5 $\mu\text{s}$ ;

4. a 4-pole, 50Hz, 1.1kW induction servomotor, whose data are listed in the appendix A;

5. a vector controlled permanent magnet synchronous motor used to provide the load torque.

The motor position and speed are measured by means of a 512 pulse/revolution incremental encoder. The sampling time for the controller is set to 200 $\mu\text{s}$ . In order to get the discrete time version of control algorithm the simple Euler method is used. Two stator phase currents, simultaneously and synchronously sampled at the symmetry point of the PWM signals, in order to filter out the modulation ripple, are measured by Hall-effect zero field sensors, only for monitoring purposes.

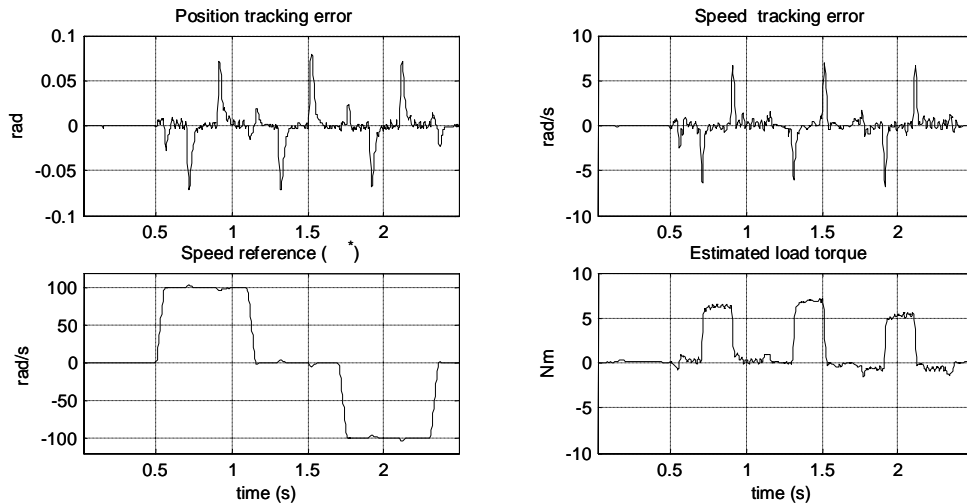


Fig. 2. Dynamic behaviour of the position controller.

error is about 7 rad/s during constant load torque rejection and of about 2 rad/s during reference trajectory tracking. A settling time of about 80 ms during step load torque rejection is obtained. Note that phases with constant speed reference and constant load torque, steady state position tracking error is zero. Torque current required during transients and during load torque rejection is equal to the nominal value. It is worth observing that negligible current regulation errors are present during the experiments, despite of imperfect knowledge of the induction motor parameters (e.g. due to thermal drift in the value of stator and rotor resistance) and plant nonidealities, such as the inverter ones. In particular, dead time effect has not been compensated in the control algorithm. Dead time introduces error mostly at zero or low speed in the d-axis current.

The experimental tests were carried out using a rapid prototyping station (RPS), which includes:

1. a Personal Computer acting as the Operator Interface during the experiments;
2. a custom floating-point digital signal processor

Experimental results, reported in Figs. 2, 3 and 4, have been performed in order to test the dynamic performance of the control algorithm during position trajectory tracking and load torque rejection. The transient performance is characterized by a maximum position error of about 0.02 rad during reference trajectory tracking and about 0.07 rad during constant rated load torque rejection. Maximum speed

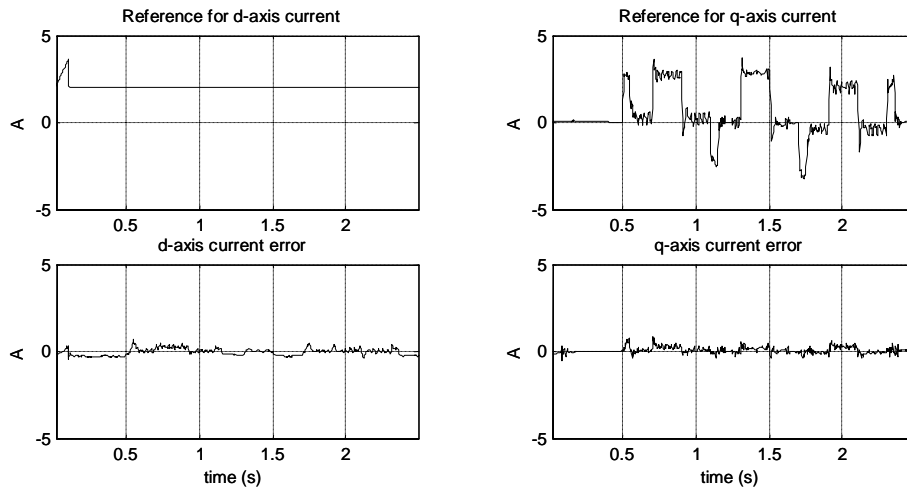


Fig. 3. Dynamic behaviour of the position controller.

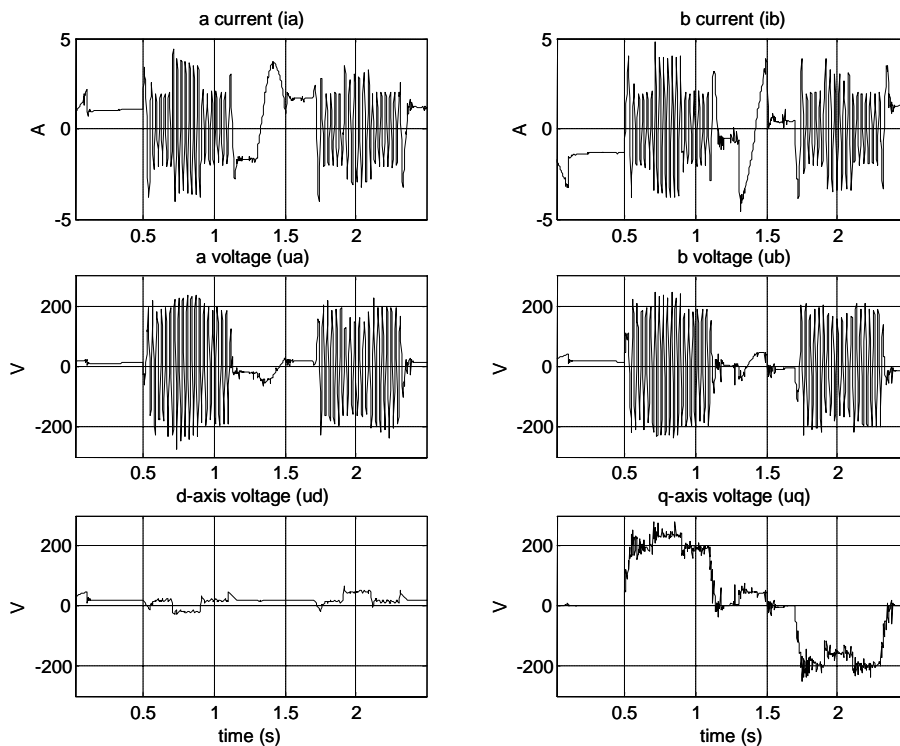


Fig 4. Dynamic behaviour of the position controller

## 6. Conclusions

A new stator sensorless position-flux tracking control algorithm is presented. It is based on concept of natural indirect field-orientation and provides global asymptotic position and rotor flux modulus tracking in presence of constant unknown load torque. Experimental results proof a level of achievable performance suitable for wide spectrum of technological servo applications.

## Appendix

Nominal parameters of the induction motor adopted for the experimental test

Rated power	1.1kW	Excitation current	1.4 A	Magnetization inductance	0.434 H
Rated torque	7.0Nm	Rated current	2.8 A	Stator inductance	0.48 H
Rated frequency	50Hz	Stator resistance	10.2 $\Omega$	Rotor inductance	0.46 H
Number of poles	2	Rotor resistance	4.8 $\Omega$	Total inertia	0.0034 Kgm <sup>2</sup>

## References

- [1] D.W. Novotny, T.A. Lipo, *Vector Control and Dynamics of AC Drives*. Oxford, U.K.: Oxford Univ. Press, 1996
- [2] W. Leohnard, *Control of Electric Drives*. Berlin, Germany: Springer-Verlag, 1995
- [3] M. Feemster, P. Vadagarbha, D. Haste, D.M. Dawson, "Adaptive output-feedback control of induction motors", *Proc. 36<sup>th</sup> IEEE Decision and Control Conf.*, vol. 2, pp. 1950-1955, 10-12 Dec. 1997
- [4] S. Peresada, A. Tonielli, "High-performance robust speed-flux tracking controller for induction motor", *Int. J. Adapt. Control Signal Process.*, vol. 14, pp. 177-200.